Excitation spectrum and magnetic field effects in a quantum critical spin-orbital system: The case of $FeSc_2S_4$

Gang Chen
Physics Department, University of California, Santa Barbara, California 93106, USA

Andreas P. Schnyder and Leon Balents
Kavli Institute for Theoretical Physics, University of California, Santa Barbara, California 93106, USA

(Received 9 July 2009; published 7 December 2009)

The orbitally degenerate A-site spinel compound $FeSc_2S_4$ has been experimentally identified as a "spin-orbital liquid," with strong fluctuations of both spins and orbitals. Assuming that the second-neighbor spin-exchange J_2 is the dominant one, we argued in a recent theoretical study [G. Chen *et al.*, Phys. Rev. Lett. **102**, 096406 (2009)] that $FeSc_2S_4$ is in a local "spin-orbital singlet" state driven by spin-orbit coupling, close to a quantum critical point, which separates the spin-orbital singlet phase from a magnetically and orbitally ordered phase. In this paper, we refine further and develop this theory of $FeSc_2S_4$. First, we show that inclusion of a small first-neighbor exchange J_1 induces a narrow region of incommensurate phase near the quantum critical point. Next, we derive the phase diagram in the presence of an external magnetic field B, and show that the latter suppresses the ordered phase. Lastly, we compute the field-dependent dynamical magnetic susceptibility $\chi(\mathbf{k},\omega;B)$, from which we extract a variety of physical quantities. Comparison with and suggestions for experiment are discussed.

DOI: 10.1103/PhysRevB.80.224409 PACS number(s): 71.70.Ej, 71.70.Gm, 75.10.−b, 75.40.−s

I. INTRODUCTION

Among all the magnetic spinels,[1–13] the A-site spinel $FeSc_2S_4$ is particularly intriguing in that its frustration parameter[14,15] $f \gtrsim 1000$ is one of the largest ever reported.[5–7] Indeed, even though the material clearly exhibits well-formed local moments interacting with a characteristic energy given by the Curie-Weiss temperature $|\Theta_{CW}|=45$ K, no sign of magnetic ordering has been found down to the lowest measurable temperature of 50 mK. Moreover, $FeSc_2S_4$ is interesting because it has not only spin but also orbital degeneracy. The Fe^{2+} ion at the A-site is in a $3d^6$ configuration, whose fivefold degeneracy is split by the tetrahedral crystal field into a lower e_g doublet and an upper t_{2g} triplet. The six electrons in the $3d$ shell are Hund's rule coupled, yielding a high spin configuration with $S=2$ and a twofold orbital degeneracy due to a hole in the lower e_g doublet. Besides the fivefold spin degeneracy and the lattice degrees of freedom, the orbital degeneracy gives an additional contribution to the specific heat. This has been confirmed experimentally.[6,7]

Commonly, orbital degeneracies are relieved by a Jahn-Teller-type structural distortion, that leads to orbital order at low temperatures. However, in $FeSc_2S_4$ no such distortion has been observed. Hence, both the spins and orbitals remain frustrated and continue to fluctuate down to the lowest measured temperature, a situation for which the term "spin orbital liquid" (SOL) was coined. A SOL state was also suggested for $LiNiO_2$.[16,17] But this proposal has been questioned recently in Ref. 18, where it was argued that the unusual behavior of $LiNiO_2$ is due to disorder effects. Therefore $FeSc_2S_4$ remains as the best candidate for a SOL.

In an undistorted lattice, exchange interactions or spin-orbit coupling can split the orbital and spin degeneracies of a single Fe^{2+} ion. To study these possibilities we introduced in Ref. 19 a model that contains a "Kugel-Khomskii"-type[20] spin-orbital exchange interaction as well as the lowest-order symmetry-allowed atomic spin-orbit coupling. The exchange interactions favor spin and orbital order whereas the on-site spin-orbit coupling leads to the formation of a local "spin-orbital singlet" (SOS). In $FeSc_2S_4$ there is strong competition between these two interactions. We argued in Ref. 19 that $FeSc_2S_4$ is in the SOS state, close to a quantum critical point (QCP) that separates the SOS phase from the ordered phase (see Fig. 1). This QCP seems to be rather analogous to that appearing in spin-dimer materials[21,22] or bilayer Heisenberg models,[23] with the two orbital states playing the roles of the two members of a spin dimer or the two bilayer states. However, we will discover at least one surprising difference below.

Previously, we have argued that, to a first approximation, $FeSc_2S_4$ can be described by a simplified "J_2-λ model,"[19]

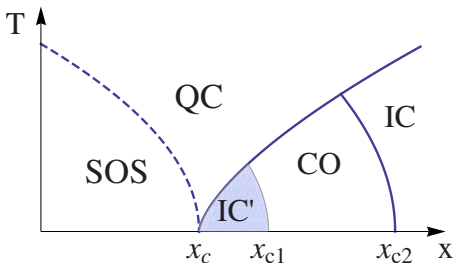

FIG. 1. (Color online). Phase diagram as a function of temperature T and x, the ratio of exchange to spin-orbit interaction. A QCP at x_c separates the SOS state from the ordered phase. Within the order phase, at x_{c2}, there is a commensurate-incommensurate phase transition. "QC" denotes the quantum critical regime, "CO" the commensurate antiferromagnet with orbital order, and "IC" the incommensurate spin and orbital order. Inclusion of a small first-neighbor exchange J_1 induces a second region of incommensurate phase (shaded area).

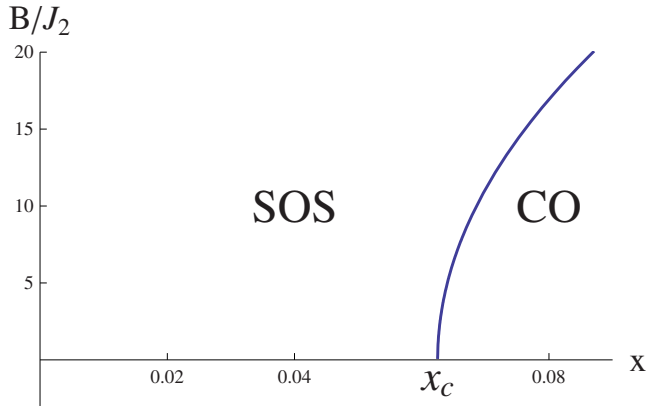

FIG. 2. (Color online). Phase diagram of the J_2-λ model, Eq. (14), as a function of magnetic field B and coupling ratio x. In zero magnetic field the phase transition between the SOS phase and the CO state occurs at $x_c=1/16$.

which only contains on-site spin-orbit and next-nearest-neighbor (NNN) spin-exchange interactions. Within this approximation the two fcc sublattices of the A-site diamond lattice decouple completely. The aim of the present paper is to refine the model of Ref. 19 and to calculate more detailed physical properties for comparison with experiments.

We summarize the results here. We first consider the effects of weak intersublattice nearest-neighbor (NN) exchange J_1. We find that it induces a narrow range of *incommensurate* magnetically ordered phase in the vicinity of the QCP, on the ordered side (see Fig. 1). Next, we consider the effects of an external magnetic field B on the QCP in the J_2-λ model. Quite surprisingly, we find that the magnetic field *destroys* the spin order and the QCP shifts from $x_c=1/16$ to a larger value (see Fig. 2). This is exactly the *opposite* trend to that observed in the spin-dimer and bilayer models. Within mean-field theory we calculate both the uniform and staggered magnetization as a function of B. Finally, we use the random-phase approximation (RPA) to compute the field-dependent dynamical spin susceptibility Im $\chi(\boldsymbol{k},\omega,B)$ in the SOS phase. From an analysis of the pole structure of $\chi(\boldsymbol{k},\omega)$ we obtain the dispersion of the low-energy collective modes. Consistent with the effect of the magnetic field on the phase diagram, we find that the gap in the SOS phase increases with B.

The remainder of the paper is organized as follows. In Sec. II, we define the model Hamiltonian and summarize the principal results of Ref. 19. The weak intersublattice interaction is introduced in Sec. III, where we derive the resulting changes to the phase diagram. In Sec. IV, we return to the minimal NNN model but include the effects of an external magnetic field. The inelastic structure factor (dynamical spin susceptibility) is calculated by the RPA approximation in Sec. V. We conclude with a summary and discussion in Sec. VI. Some technicalities are given in the Appendix.

II. MODEL DEFINITION

The Hamiltonian contains two terms: an exchange interaction $\mathcal{H}_{\rm ex}$ and an atomic spin-orbit coupling $\mathcal{H}_0^i$,

$$\mathcal{H}=\mathcal{H}_{\rm ex}+\sum_i \mathcal{H}_0^i. \tag{1a}$$

The term $\mathcal{H}_{\rm ex}$ describes spin and orbital exchange interactions as well as couplings between spin and orbital degrees of freedom. Using microscopic considerations and symmetry constraints one can show that $\mathcal{H}_{\rm ex}$ is of the form[19]

$$\mathcal{H}_{\rm ex}=\frac{1}{2}\sum_{ij}[J_{ij}\mathbf{S}_i\cdot\mathbf{S}_j+2K_{ij}\mathbf{T}_i\cdot\mathbf{T}_j(4+\mathbf{S}_i\cdot\mathbf{S}_j)], \tag{1b}$$

where $\mathbf{S}_i$ is the $S=2$ spin operator at site i. The orbital degrees of freedom are described by $T=1/2$ pseudospin operators $\mathbf{T}_i$ that act on the x^2-y^2 and $3z^2-r^2$ orbitals in the e_g subspace. An analysis of the exchange paths linking two A sites shows that both first- and second-neighbor exchange paths are of comparable length and have similar multiplicity.[7,24] This suggests that there is a substantial NNN interaction and it is therefore necessary to keep in Eq. (1b) the sum over both the NN and NNN sites. For convenience we set $J_{ij}=J_1$ or J_2 when ij are first- and second-neighbor sites, respectively (and similarly for K_{ij}).

The second term in Eq. (1a), $\mathcal{H}_0^i$, is the on-site spin-orbit coupling which arises from second-order perturbation theory,[25]

$$\mathcal{H}_0^i=-\frac{\lambda}{3}\{\sqrt{3}T_i^x[(S_i^x)^2-(S_i^y)^2]+T_i^z[3(S_i^z)^2-\mathbf{S}_i^2]\}, \tag{1c}$$

where the coefficient λ is estimated from microscopic atomic calculations to be $\lambda\simeq 6\lambda_0^2/\Delta_{\rm te}$. Here, λ_0 denotes the atomic spin-orbit interaction and $\Delta_{\rm te}$ is the energy separation between the e_g and t_{2g} states. Note, that $\mathcal{H}_0^i$ immediately leads to a splitting of the ionic degeneracies because the ground state of $\mathcal{H}_0^i$ is the nondegenerate spin-orbital singlet,

$$\frac{1}{\sqrt{2}}|x^2-y^2\rangle|S^z=0\rangle+\frac{1}{2}|3z^2-r^2\rangle[|S^z=+2\rangle+|S^z=-2\rangle]. \tag{2}$$

Whether $FeSc_2S_4$ is in such a SOS phase depends on the ratio between exchange and on-site spin-orbit interactions,

$$x\equiv\max\{J_1,J_2,K_1,K_2\}/\lambda. \tag{3}$$

We note that we have *not* included spin-orbit effects such as Dzyaloshinskii-Moriya interactions in the exchange Hamiltonian, Eq. (1b). This may be surprising since the on-site spin-orbit coupling in Eq. (1c) plays a crucial role in our analysis. However, we expect that the spin-orbit corrections to the exchange are smaller than the leading-order exchange couplings by a factor of order λ_0/Δ_{te}. Using the numbers of Ref. 19, $\lambda_0\sim 80$ cm^{-1} and $\Delta_{te}\sim 2500$ cm^{-1}, this yields the Dzyaloshinskii-Moriya interaction $D\sim 0.032J_2$. This makes them subdominant both to the isotropic exchange couplings in Eq. (1b) and the on-site spin-orbit interaction in Eq. (1c), which are comparable in $FeSc_2S_4$(this indeed defines the location of the QCP—see below).

From a comparison with experiments we showed in Ref. 19 that J_2 is antiferromagnetic and the largest among all the exchange-coupling constants, whereas λ is competitive, but slightly larger than the NNN spin-exchange interaction J_2.

This observation leads us to consider a "minimal" version of model (II), which only includes the NNN spin-exchange J_2 and the on-site spin-orbit interaction λ (i.e., $J_1=K_1=K_2=0$). Within this J_2-λ model we demonstrated that $FeSc_2S_4$ is in the SOS phase close to the QCP of Fig. 1.

The full phase diagram of Hamiltonian (1) as a function of temperature and ratio x, Eq. (3), includes a commensurate-incommensurate transition within the ordered phase (see Fig. 1). Deep in the ordered phase when the exchange interactions are dominant ($x \gg 1$) the incommensurate spin and orbital order (IC) is generally favored by the exchange Hamiltonian (1b). With the inclusion of weak spin-orbit interaction, Eq. (1c), i.e., with decreasing x, the spin and orbital order becomes commensurate with the spins and orbitals both forming a spiral with wave vectors $\mathbf{p}=2\pi(1,0,0)$ and $\mathbf{q}=(0,0,0)$, respectively.

III. EFFECTS OF WEAK INTERSUBLATTICE SPIN-EXCHANGE INTERACTION

As mentioned in Sec. I, the inclusion of a small NN interaction J_1 induces a narrow region of incommensurate order near the QCP (shaded area in Fig. 1). In this section we give a derivation of this results using a Landau expansion of the effective action.

First, we note that the Hamiltonian in Eq. (14) has independent cubic "internal" spin symmetry and cubic "external" space-group symmetry. We therefore have the symmetry-allowed free energy for two decoupled fcc sublattices[19] near the QCP,

$$\begin{aligned} f_0[(\psi)] = & \sum_{\mu=A,B;a} \left(v_1^2 |\partial_a \boldsymbol{\psi}_{\mu,a}|^2 + v_2^2 \sum_{b\neq a} |\partial_b \boldsymbol{\psi}_{\mu,a}|^2 + r|\boldsymbol{\psi}_{\mu,a}|^2 \right) \\ & + g_1 \sum_{\mu,a} (|\boldsymbol{\psi}_{\mu,a}|^2)^2 + g_2 \sum_{\mu,a,b} (\psi^b_{\mu,a})^4 \\ & + \sum_{\mu} \mathrm{Sym}\, [g_3 (\psi^x_{\mu,1})^2 (\psi^x_{\mu,2})^2 + g_4 (\psi^x_{\mu,1})^2 (\psi^y_{\mu,2})^2 \\ & + g_5 \psi^x_{\mu,1} \psi^y_{\mu,1} \psi^x_{\mu,2} \psi^y_{\mu,2}]\}, \end{aligned} \tag{4}$$

where the order parameters $\psi_{\mu,a}$ are the (real) staggered magnetizations introduced by

$$\langle \mathbf{S}_i \rangle = \begin{cases} \sum_{a=x,y,z} \boldsymbol{\psi}_{A,a} (-1)^{2x_i^a} & i \in \mathrm{A\ \ sublattice} \\ \sum_{a=x,y,z} \boldsymbol{\psi}_{B,a} (-1)^{2x_i^a} & i \in \mathrm{B\ \ sublattice} \end{cases} \tag{5}$$

and x_i^a are the canonical half-integer coordinates of the fcc lattice with the cubic supercell having unit length. For our convenience we choose the same set of fcc coordinates for the two sublattices. In Eq. (4), "Sym" indicates symmetrization with respect to both wave vector (lower) and spin (upper) indices.

We now introduce weak intersublattice interactions. As a result, extra terms which couple two fcc sublattices will appear in Eq. (4). By the symmetry analysis, we obtain the intersublattice terms,

$$f_{\mathrm{int}}(\{\psi\}) = \sum_a \gamma \boldsymbol{\psi}_{A,a} \partial_a \boldsymbol{\psi}_{B,a} - \eta (\boldsymbol{\psi}_{A,a} \cdot \boldsymbol{\psi}_{B,a})^2, \tag{6}$$

where we have kept the leading quadratic term (others have more derivatives) and the most important quartic term, which is when intersublattice couplings first appear without derivatives. A number of other quartic couplings involving the two sublattices are also allowed but do not play any important role in what follows.

We now proceed to analyze the Landau theory of Eqs. (4) and (6). First consider the behavior on approaching the QCP from the SOS phase. The first instability of the SOS phase is signaled by the quadratic part of the action alone, i.e., the vanishing of the lowest eigenvalue of the associated quadratic form. Due to the linear derivative term, the unstable eigenvectors are nonconstant fields of the form

$$\begin{aligned} \psi^b_{A,a} &= \psi^b_a \cos(\delta x_a + \theta_{a,b}), \\ \psi^b_{B,a} &= \psi^b_a \sin(\delta x_a + \theta_{a,b}) \end{aligned} \tag{7}$$

with $\delta=\gamma/(4v_1^2)$, and $\psi^b_a, \theta_{a,b}$ arbitrary constants. There is one linearly independent unstable eigenvector for each a and b. The particular form of superposition which is favored in the ordered state is determined by the quartic terms. We expect on physical grounds that the ordered states will be of spiral type, with approximately constant *magnitude* of spin expectation values, and with a "single q" structure. The latter condition means that $\boldsymbol{\psi}_{A,a}$ is nonzero only for a single $a=x$, y, *or* z. A sufficient condition for a single q structure to be favored is that $g_3, g_4, g_5 > 0$ (though this condition can be relaxed somewhat). In this case, we have

$$\begin{aligned} \boldsymbol{\psi}_{A,a} &= \psi_0\, \mathrm{Re}[(\hat{\mathbf{e}}_1 + i\hat{\mathbf{e}}_2) e^{i(\delta x_a + \theta)}], \\ \boldsymbol{\psi}_{B,a} &= \psi_0\, \mathrm{Re}[(-\hat{\mathbf{e}}_2 + i\hat{\mathbf{e}}_1) e^{i(\delta x_a + \theta)}]. \end{aligned} \tag{8}$$

This corresponds to an incommensurate spiral state of spins with the wave vector

$$\mathbf{p} = (2\pi \pm \delta)(1,0,0). \tag{9}$$

The unit vectors $\hat{\mathbf{e}}_{1/2}$ define the plane in which the spins rotate. At the quadratic level, this plane is arbitrary but it will be selected by the quartic terms in the free energy. Presuming that the system has axial cubic anisotropy (preferring spins aligned with the x, y, or z axes), a (100) or symmetry-related plane will be chosen. This is controlled in the free energy by the coefficient g_2, which should be negative to mimic axial cubic anisotropy.

Now consider the evolution of the spin configuration as the system becomes more strongly ordered. As $|\boldsymbol{\psi}|$ increases, we expect the quartic terms in the free energy to become more important, favoring commensurate states in which the spins are aligned with the principal axis. To analyze how this occurs, we presume that the spins remain in a single q structure (a spiral rather than a more exotic "spin lattice") so that $\boldsymbol{\psi}_{\mu,a}$ is nonzero only for one a. Furthermore, we assume that the spins remain in a single (100) plane. Up to symmetry-related choices we take $a=x=1$, and $\hat{\mathbf{e}}_1=\hat{\mathbf{x}}, \hat{\mathbf{e}}_2=\hat{\mathbf{y}}$ in Eq. (7).

Finally, we presume that the fields depend only upon x, as can be easily verified is true for the minimum free-energy configurations.

Inserting this into Eqs. (4) and (6) and assuming ψ_0 is constant, we obtain the reduced free-energy density, neglecting an additive constant

$$f = \frac{\kappa}{2}(\partial_x \theta)^2 + \sigma \cos 4(\theta + \delta x) \tag{10}$$

with $\kappa = 4v_1^2\psi_0^2$ and $\sigma = g_2\psi_0^4/2$. This is a standard sine-Gordon model, with incommensuration δ. It describes a competition between a commensurate state in which $\theta + \delta x$ is constant and an incommensurate one in which $\partial_x\theta < \delta$ on average. The transition between the two states is known as a commensurate-incommensurate-transition (CIT), and its location is determined by the condition that the energy of a single domain-wall excitation of the commensurate state (a "soliton") vanishes. In this way we can precisely determine the location of the CIT. We find that the CIT occurs for[26]

$$\delta_c = \frac{2}{\pi}\sqrt{\frac{|\sigma|}{\kappa}}. \tag{11}$$

When $\delta < \delta_c$, the system is in a commensurate state.

We must now translate this condition back to obtain the critical point in terms of microscopic parameters x, x_c, and J_1/J_2. In Appendix, we determine the necessary coefficients in Eqs. (4) and (6) $(v_1^2, r, g_1, g_2, \gamma)$ by deriving the effective action by standard Hubbard-Stratonovich methods from the microscopic spin-orbital Hamiltonian. The results are given in Eqs. (A8) and (A9). In addition, we require the amplitude ψ_0 to minimize the free energy. With this we can calculate κ and σ, and hence solve Eq. (11) for the location of the CIT. To get the amplitude, we recognize that at the CIT the solution is commensurate, i.e., has the form of Eq. (8) with $\delta = \theta = 0$. Therefore, we may simply evaluate the free energy in Eq. (4) using this form of the order parameter, and minimize over ψ_0. The result is that

$$\psi_0^2 = \frac{-r}{2(g_1 + g_2)}, \tag{12}$$

where at the CIT of course $r < 0$. Combining the above results, we obtain the CIT transition point

$$x_{c1} = \frac{1}{16}\left[1 + \frac{\pi^2}{4}\left(\frac{J_1}{J_2}\right)^2\right] \tag{13}$$

for $J_1 \ll J_2$. As expected, for small J_1, the incommensurate phase studied here is narrow and located only near the QCP (see Fig. 1). As discussed in Ref. 19, a different incommensurate phase arises for much larger J_2, when the spin-orbit interaction plays a minimal role. This transition to the second incommensurate phase occurs at $x_{c2} \approx 0.61(J_2/J_1)^2$, far from the QCP.

IV. J_2-λ MODEL IN A MAGNETIC FIELD

In this section we study the minimal J_2-λ model in an external magnetic field B both in the commensurate ordered (CO) and the SOS phases (see Fig. 1). For definiteness we assume that the spins in the CO phase align themselves along the x axis whereas the magnetic field is applied along the z axis. We use mean-field theory to calculate the uniform and staggered magnetizations and derive therefrom the magnetic phase diagram of the J_2-λ model.

The minimal J_2-λ model in an external magnetic field B contains only on-site and NNN interactions. Therefore the diamond lattice decomposes into two fcc sublattices with J_2 playing the role of the NN exchange interaction within each sublattice. The Hamiltonian is

$$\mathcal{H}_{\min} = \sum_{\langle ij \rangle} J_2 \mathbf{S}_i \cdot \mathbf{S}_j + \sum_i \mathcal{H}_0^i + B\sum_i S_i^z, \tag{14}$$

where $\langle ij \rangle$ represents nearest-neighbor sites on an fcc sublattice and $\mathcal{H}_0^i$ is defined by Eq. (1c). In the absence of a magnetic field and when $J_2/\lambda > x_c = 1/16$ the system is in the CO phase[19] with the spins aligned antiferromagnetically along one of the three cubic axes (here taken to be the x axis). To decouple the exchange interaction in Eq. (14) we employ mean-field theory with the following ansatz for the average spin at site i,

$$\langle \mathbf{S}_i \rangle = n \cos(\mathbf{p} \cdot \mathbf{r}_i)\hat{x} + m\hat{z}. \tag{15}$$

Here, m and n denote uniform and staggered magnetizations, respectively, and $\mathbf{r}_i$ are the usual half-integer coordinates of the fcc sites. In the CO state the spiral momentum takes the form $\mathbf{p} = 2\pi(1,0,0)$ thereby encoding the antiferromagnetic order along the x axis. In the disordered SOS phase the staggered moment is vanishing, $n = 0$. With this, the resulting single-site mean-field Hamiltonian reads

$$\mathcal{H}_i^{\mathrm{MF}} = h_z S_i^z + h_x S_i^x + \mathcal{H}_0^i, \tag{16a}$$

where we have introduced the two effective magnetic fields,

$$h_z \equiv 12J_2 m + B, \quad h_x \equiv -4J_2 n. \tag{16b}$$

At zero temperature the self-consistent mean-field equations for the uniform and staggered magnetizations are given by

$$m = \frac{\partial \epsilon(h_x, h_z)}{\partial h_z}, \tag{17a}$$

$$n = \frac{\partial \epsilon(h_x, h_z)}{\partial h_x}, \tag{17b}$$

where $\epsilon(h_x, h_z)$ denotes the ground-state energy of the mean-field Hamiltonian (16). The numerical solutions to these equations are presented in Fig. 3. We find that with increasing field the staggered magnetization is suppressed, and eventually the magnetic order is destroyed. Hence, the critical coupling ratio x_c moves from $x_c = 1/16$ to larger values with increasing field (see Fig. 2). The uniform magnetization shows a small "shoulder" at the critical magnetic field when the staggered magnetization vanishes.

In the neighborhood of the QCP ($|x/x_c - 1| \ll 1$) and for B small compared to J_2 it is legitimate to expand the ground-state energy $\epsilon(h_x, h_z)$ in the effective magnetic fields h_x and h_z. Up to fourth order we have

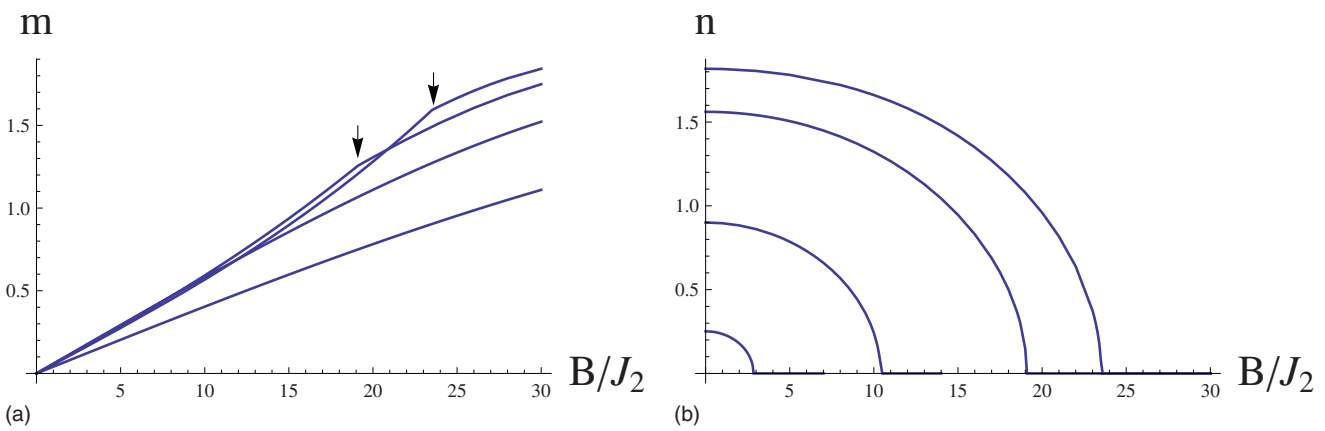

FIG. 3. (Color online). (a) Uniform magnetization m versus magnetic field B (in units of the spin-exchange J_2) for different coupling ratios x (from top to bottom $x=0.15, 0.10, 0.05, 0.02$, respectively). The arrows indicate the position of the QCP. (b) Staggered magnetization n as a function of B (in units of the spin-exchange J_2) for $x=0.15, 0.10, 0.07, 0.063$ (from top to bottom curve).

$$\epsilon(h_x,h_z) \simeq -2\lambda - \frac{2}{\lambda}(h_x^2+h_z^2) + \frac{2}{\lambda^3}(h_x^4+4h_x^2h_z^2+h_z^4). \tag{18}$$

Neglecting terms of order h_z^3 and higher, we obtain the following expressions for the uniform magnetization:

$$m = \begin{cases} -\dfrac{4B}{48J_2+\lambda}, & \text{SOS} \\ -\dfrac{(8J_2-\lambda)B}{2J_2(48J_2-7\lambda)}, & \text{CO} \end{cases} \tag{19}$$

in the SOS and CO phases, respectively. Similarly, the staggered magnetization is given by

$$n = \begin{cases} 0, & \text{SOS} \\ 8\sqrt{2[x-x_c(B)]}, & \text{CO} \end{cases} \tag{20}$$

with

$$x_c(B) = \frac{1}{16} + \frac{B^2}{16384J_2^2}, \tag{21}$$

where we retained only the lowest-order term in B. The approximate result for the uniform magnetization, Eq. (19), describes the linear dependence on magnetic field in the regime where B is small compared to J_2 (cf. Fig. 3). It is interesting to note that this behavior agrees with the measured low-temperature magnetic susceptibility in $FeSc_2S_4$. Indeed, it is found in Ref. 7 that the magnetic susceptibility in $FeSc_2S_4$ at $T\to 0$ saturates to a constant value, independent of B.

To conclude, we find that an external magnetic field leads to a suppression of spin ordering. On the ordered side of the QCP there is a phase transition to the disordered SOS phase as the magnetic field is increased. This behavior is quite different from a *spin* singlet phase in a typical spin-only system such as $TlCuCl_3$ (Ref. 21) or $BaCuSi_2O_6$,[22] where only the magnetic triplet excited states—magnons—respond to the magnetic field whereas the nonmagnetic singlet ground state is unaffected. Hence, the field stabilizes spin order by Bose-Einstein condensation of magnons. Here, however, the strong spin-orbit interaction leads to very different physics. Specifically, SOS is not a spin singlet but a highly entangled quantum state of spin and orbital degrees of freedom. As a consequence, it responds strongly to the applied field and indeed takes better advantage of the field than does the ordered Néel state.

V. DYNAMICAL SPIN SUSCEPTIBILITY AND ENERGY GAPS

In this section, we compute the dynamical spin susceptibility in the SOS phase with the exchange coupling J_2 treated within the RPA. This could be compared to inelastic neutron-scattering data. The energy gaps to the low-lying collective modes are derived from an analysis of the pole structure of the dynamical spin susceptibility.

In the SOS phase we can approximate the full magnetic susceptibility of the J_2-λ model $\chi^{\mu\nu}(\mathbf{k},\omega;B)$ by the RPA in terms of the noninteraction susceptibility $\chi_0^{\mu\nu}(\boldsymbol{k},\omega,B)$ of the on-site Hamiltonian $\mathcal{H}_0^i+BS_i^z$ [see Eq. (1c)]. For the xx component we have

$$\chi^{xx}(\mathbf{k},\omega;B) = \frac{\chi_0^{xx}(\omega)}{1-\mathcal{J}(\mathbf{k})\chi_0^{xx}(\omega)}, \tag{22}$$

where $\mathcal{J}(\mathbf{k})$ is the Fourier transform of the exchange coupling,

$$\mathcal{J}(\mathbf{k}) = \sum_{\{\mathbf{A}\}} J_2 \cos(\mathbf{k}\cdot\mathbf{A}) \tag{23}$$

with $\{\mathbf{A}\}$ denoting the 12 NNN lattice vectors. The single-site spin susceptibility $\chi_0^{xx}(\omega;B)$ can be constructed from the spectral representation. At zero temperature $\chi_0^{xx}(\omega;B)$ is given by

$$\chi_0^{xx}(\omega;B) = \sum_{j\neq 0}\left[\frac{|\langle 0|S^x|j\rangle|^2}{\epsilon_j-\omega-i\Gamma} + \frac{|\langle 0|S^x|j\rangle|^2}{\epsilon_j+\omega+i\Gamma}\right], \tag{24}$$

where $|0\rangle$ and $|j\rangle$ are the ground state and excited states of the on-site term $\mathcal{H}_0^i+BS_i^z$, respectively. The energy difference between the excited state $|j\rangle$ and the ground state $|0\rangle$ is de-

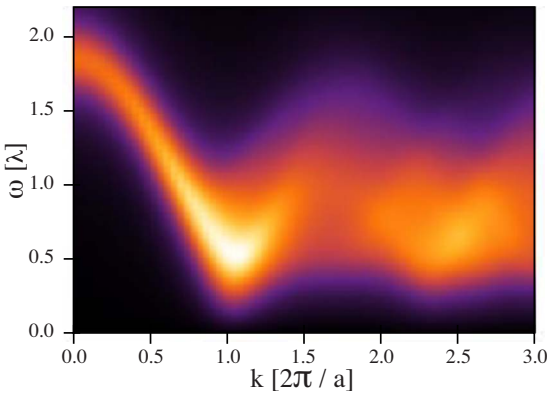

FIG. 4. (Color online) Imaginary part of the angular-averaged RPA spin susceptibility in zero magnetic field Im $\chi^{xx}_{\mathrm{av}}(k,\omega;0)$ with $J_2/\lambda=0.05$ and a damping $\Gamma/\lambda=0.2$.

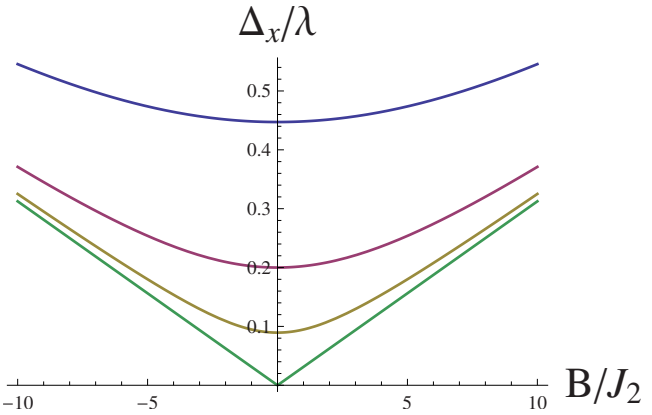

FIG. 5. (Color online). Energy gap Δ_x (in units of the spin-orbit coupling λ) as a function of magnetic field (in units of the spin-exchange J_2) for different coupling ratios x (from top to bottom $x=0.05, 0.06, 0.062, 1/16$).

noted by ϵ_j. Finite lifetime effects are parametrized by a phenomenological damping $\Gamma>0$. In order to facilitate a direct comparison with neutron-scattering data on polycrystalline samples we perform a numerical average of $\chi^{xx}(\mathbf{k},\omega;B)$ over the angular components of the wave vector $\boldsymbol{k}$. For a given wave-vector magnitude $k=|\boldsymbol{k}|$ we define the angular-averaged spin susceptibility by

$$\chi^{xx}_{\mathrm{av}}(k,\omega;B)=\int \sin\theta d\theta d\phi \chi^{xx}(\boldsymbol{k},\omega;B), \tag{25}$$

where θ and ϕ describe the direction of the wave vector $\boldsymbol{k}$. Since the inelastic neutron-scattering intensity is proportional to the imaginary part of $\chi^{xx}_{\mathrm{av}}(k,\omega;B)$ we compute Im $\chi^{xx}_{\mathrm{av}}(k,\omega;B)$ as a function of energy transfer ω and wave-vector magnitude k. Figure 4 displays the numerically calculated dynamical spin susceptibility Im $\chi^{xx}_{\mathrm{av}}(k,\omega;0)$ in zero magnetic field. The excitation minima near $k=2\pi/a$ and $k=5\pi/a$ agree well with the neutron-scattering data on polycrystalline samples.[5]

The dispersing excitation branch shown in Fig. 4 is a collective mode associated with zeros of the real part of the denominator in Eq. (22). For the unaveraged dynamical spin susceptibility Im $\chi^{xx}(\boldsymbol{k},\omega,B)$ the frequency minimum Δ_x of the dispersing collective mode occurs at $\mathbf{k}=2\pi(1,0,0)$. Upon approaching the QCP from the disordered side and for small magnetic field B we find that the gap Δ_x is vanishing as

$$\Delta_x=4\lambda\sqrt{x_c(B)-x}, \tag{26}$$

where $x_c(B)$ is defined by Eq. (21). [The same result also holds for the energy minimum Δ_y of the collective mode described by Im $\chi^{yy}(\mathbf{k},\omega;B)$.] Figure 5 depicts the gap Δ_x, Eq. (26), as a function of magnetic field for different coupling ratios x in the SOS phase.

VI. DISCUSSION

A. Summary

In this work we have refined the theory, developed in Ref. 19, of the QCP in a spin-orbital Hamiltonian for the A-site spinel compound $FeSc_2S_4$. The model exhibits an interesting quantum critical point; on increasing the second-neighbor spin-exchange interaction J_2 it passes through a zero-temperature phase transition from a spin-orbital singlet state to a magnetically and orbitally ordered phase. First, we considered the effects of a weak nearest-neighbor exchange interaction J_1, which induced a narrow region of incommensurate phase near the QCP. We studied the associated commensurate-incommensurate transition. Next, we included the effects of an external magnetic field. While the quantum critical point studied here seems similar to the one found in, e.g., bilayer Heisenberg antiferromagnets, its behavior under an external magnetic field is quite different. Namely, we found that a magnetic field suppresses magnetic and orbital order, and a transition from the ordered state to the spin-orbital singlet phase occurs at some critical-field strength (see Fig. 2). From these findings, we conclude that $FeSc_2S_4$, which is close to the quantum critical point, but in the spin-orbital singlet phase, does not show any field-induced transition to an ordered state. Indeed, recent NMR experiments in fields up to 8.5 T showed no signs of magnetic ordering.[10] Furthermore, we computed the dynamical spin susceptibility in the SOS phase by means of a random-phase approximation. Averaging our results over the angular components of the wave vector we performed a comparison with available neutron-scattering data on polycrystalline $FeSc_2S_4$ samples and found reasonable agreement (see Fig. 4).

B. Experiments

1. Magnetic probes

The theory exposed in this paper and Ref. 19 is broadly consistent with the results of a variety of magnetic probes applied to $FeSc_2S_4$. It explains the small but nonzero spin gap measured in inelastic neutron-scattering and NMR $1/T_1$ relaxation-rate measurements, as well as the temperature dependence of the uniform magnetic susceptibility. The present calculation of the dynamical spin susceptibility matches reasonably well with experiment. The lack of field-induced

magnetic ordering is also in agreement with the calculations in this paper.

2. Specific heat and disorder

The specific-heat data on $FeSc_2S_4$ reveal several energy scales. The magnetic specific heat divided by temperature, C_m/T, exhibits a peak at $T \approx 6$ K. The integral of C_m/T exceeds the spin-only entropy $R \ln 5$, approaching instead $R(\ln 5 + \ln 2)$ for $T \gtrsim 60$ K, evidencing the twofold orbital contribution. This is quite consistent with the present model. However, the lower temperature behavior is more complex. For $T < 2$ K, experiments are fitted approximately by $C_m \sim AT + BT^{2.5}$, with the linear term dominant for $T < 0.2$ K. The latter behavior appears at odds with the indications of an energy gap of 1–2 K in neutron-scattering and NMR experiments.

A possible reconciliation of these observations is in the effects of disorder. Microscopically, we expect the dominant type of disorder to be inversion defects in which the A and B sublattice atoms are interchanged. Inversion is very common in spinels. To understand the effects of such defects, we apply general arguments based on the Landau expansion and the theory of disordered systems. These arguments depend very little upon the specific nature of the defects, other than that they are random, not very correlated, and do not break time-reversal symmetry.

These conditions lead to an important observation since the order parameters $\boldsymbol{\psi}_{\mu,a}$ are *odd* under time-reversal, disorder couples only quadratically to them. Thus impurities behave, from the point of view of critical behavior, as random bonds rather than random fields. In three dimensions, it is known that in this case both *phases* are perturbatively stable to weak impurities. However, sufficiently close to the QCP, even weak impurities become nonperturbative. More formally, random bond disorder is a *relevant* variable at the QCP. Physically, the most important effect of disorder is to locally break the degeneracy of the different ground states of the clean system within the ordered phase. For instance, a specific impurity configuration might favor the $\mathbf{p} = 2\pi(1,0,0)$ state in one region and $\mathbf{p} = 2\pi(0,1,0)$ state in another. Far from the QCP, the surface-energy cost to create a domain wall between the two states overwhelms the random energy gain, and the system remains uniform. However, close to the QCP, the surface tension becomes small and one expects the system to break into domains. Thus impurities induce a nonuniform disordered magnetic state, a "cluster spin glass," near the QCP. We expect, moreover, that this cluster spin-glass state extends slightly *past* the QCP into the region of the SOS state of the clean system. This occurs because the system lowers its energy slightly more than in the clean case, by taking advantage of the impurities locally.

This scenario provides a possible explanation of the specific-heat data. At low temperature, a T-linear specific heat is a generic feature of spin glasses. It should occur with a small coefficient A when disorder is weak. At higher temperature, one recovers approximately the intrinsic bulk clean behavior, which would be of the form $C_m \sim BT^3 f(\Delta/k_B T)$, where Δ is the energy gap and $f(\delta)$ is a monotonic scaling function satisfying $f(0) = 1$ and $f(\delta) \sim \delta^{7/2} e^{-\delta}$ for $\delta \gg 1$. The T^3 dependence is characteristic of the linearly dispersion modes at the QCP, which is cut off by the gap. It seems plausible that the experimental observed $T^{2.5}$ dependence reflects the attempt to fit such a form to a single power law. If the impurities are not too weak, it is also plausible that they modify the T^3 behavior somewhat. In any case, the overall behavior seems reasonably in line with theoretical expectations.

C. Directions for future work

The theory in this paper (and Ref. 19) appears to give a consistent explanation for the experimental results on $FeSc_2S_4$. However, there are a number of directions that could be explored in the future. It would be desirable to have a *direct* proof of the postulated spin-orbital entanglement in the ground state of $FeSc_2S_4$. Theoretical proposals and experimental studies to this end would be welcome. Given the smallness of the gap in $FeSc_2S_4$, there is a possibility that it might be driven across the QCP by pressure, which would be very exciting. Looking more broadly, it appears that the mechanism for quantum criticality described here could apply at the very least to any material with Fe^{2+} ions in a tetrahedral environment. It would be interesting to survey such compounds for signs of this physics.

ACKNOWLEDGMENTS

This work was supported by the DOE through Basic Energy Sciences under Grant No. DE-FG02-08ER46524. L.B.'s research facilities at the KITP were supported by the National Science Foundation under Grant No. NSF PHY-0551164.

APPENDIX: HUBBARD-STRATONOVICH TRANSFORMATION AND LANDAU ACTION

In this appendix, we derive the effective Landau action, Eqs. (4) and (6), from the microscopic Hamiltonian (1) using the Hubbard-Stratonovich method to decouple the exchange interactions. In this way, we can relate the coefficients in Eqs. (4) and (6) to the microscopic exchange-coupling parameters J_i and the spin-orbit coupling λ. We consider the J_1-J_2-λ model on the diamond lattice,

$$\mathcal{H} = \sum_{\langle ij \rangle} J_1 \mathbf{S}_i \cdot \mathbf{S}_j + \sum_{\langle\langle ij \rangle\rangle} J_2 \mathbf{S}_i \cdot \mathbf{S}_j + \sum_i \mathcal{H}_0^i, \tag{A1}$$

where the brackets $\langle ij \rangle$ and $\langle\langle ij \rangle\rangle$ denote the summation over first- and second-nearest neighbors, respectively. The on-site spin-orbit coupling term $\mathcal{H}_0^i$ is given by Eq. (1c). The partition function reads

$$\mathcal{Z} = \mathrm{Tr} \exp\left[-\beta \sum_{i,j} J_{ij} \boldsymbol{S}_i \cdot \boldsymbol{S}_j - \beta \sum_i \mathcal{H}_0^i \right] \tag{A2}$$

with the exchange-coupling matrix J_{ij}. Here, $J_{ij} = J_1$ or J_2, when ij connects first-neighbor or second-neighbor sites, respectively. We decouple the exchange interaction by introducing the auxiliary field ϕ_i and transforming the partition function to

$$\mathcal{Z} = \int \mathcal{D}\phi e^{\beta/2 J_{ij}^{-1} \boldsymbol{\phi}_i \cdot \boldsymbol{\phi}_j} \operatorname{Tr} e^{-\beta \Sigma_i (\mathcal{H}_0^i + \mathbf{S}_i \cdot \boldsymbol{\phi}_i)}. \tag{A3}$$

Expanding around the saddle point yields

$$\mathcal{Z} = \int \mathcal{D}\phi \exp[-\mathcal{S}_{\text{eff}}] \tag{A4}$$

with the effective action

$$\mathcal{S}_{\text{eff}} = \int_0^\beta d\tau \Bigg[-\frac{1}{2} J_{ij}^{-1} \boldsymbol{\phi}_i \cdot \boldsymbol{\phi}_j + \frac{2\partial_\tau \phi_i \cdot \partial_\tau \phi_i}{\lambda^3} - \frac{2\phi_i \cdot \phi_i}{\lambda} + 2\frac{(\phi_i \cdot \phi_i)^2 + 2(\phi_i^x \phi_i^y)^2 + 2(\phi_i^x \phi_i^z)^2 + 2(\phi_i^y \phi_i^z)^2}{\lambda^3} \Bigg]. \tag{A5}$$

Assuming $J_1 \ll J_2$ and expressing the ϕ_μ field in terms of the staggered magnetizations $\boldsymbol{\psi}_{\mu,a}$,

$$\phi_\mu(\mathbf{r}_i) = (-)^{2x_i} \boldsymbol{\psi}_{\mu,x} + (-)^{2y_i} \boldsymbol{\psi}_{\mu,y} + (-)^{2z_i} \boldsymbol{\psi}_{\mu,z}, \tag{A6}$$

we obtain the quadratic part of the free-energy density,

$$f^{(2)}[(\psi)] = \sum_{\mathbf{k}} \sum_a \left[\frac{1}{8J_2} - \frac{2}{\lambda} + \frac{1}{32J_2} \left(1 + \frac{J_1^2}{4J_2^2} \right) k_a^2 \right] (|\boldsymbol{\psi}_{A,a}(\mathbf{k})|^2 + |\boldsymbol{\psi}_{B,a}(\mathbf{k})|^2) + \frac{iJ_1}{16J_2^2} k_a \boldsymbol{\psi}_{A,a}(-\mathbf{k}) \cdot \boldsymbol{\psi}_{B,a}(\mathbf{k}). \tag{A7}$$

We note that Eq. (A7) is compatible with Eqs. (4) and (6), which we derived using symmetry considerations. By comparing the coefficients in Eqs. (4) and (6) to those in Eq. (A7) we find the following relations:

$$v_1^2 = 1/(32J_2)\left(1 + \frac{J_1^2}{4J_2^2} \right),$$

$$r = 1/(8J_2) - 2/\lambda,$$

$$\gamma = J_1/(16J_2^2). \tag{A8}$$

Similarly, expressing the quartic terms in Eq. (A5) in terms of the staggered magnetizations one can show that the coefficients g_1 and g_2 are given by

$$g_1 = 4/\lambda^3,$$

$$g_2 = -2/\lambda^3. \tag{A9}$$

[1] N. Tristan, J. Hemberger, A. Krimmel, H. A. Krug von Nidda, V. Tsurkan, and A. Loidl, Phys. Rev. B **72**, 174404 (2005).
[2] A. Krimmel, V. Tsurkan, D. Sheptyakov, and A. Loldl, Physica B (Amsterdam) **378-80**, 583 (2006).
[3] T. Suzuki, H. Nagai, M. Nohara, and H. Takagi, J. Phys.: Condens. Matter **19**, 145265 (2007).
[4] G. M. Kalvius, A. Krimmel, O. Hartmann, F. J. Litterst, R. Wappling, V. Tsurkan, and A. Loidl, Physica B (Amsterdam) **404**, 660 (2009).
[5] A. Krimmel, M. Mücksch, V. Tsurkan, M. M. Koza, H. Mutka, and A. Loidl, Phys. Rev. Lett. **94**, 237402 (2005).
[6] V. Fritsch, J. Hemberger, N. Büttgen, E.-W. Scheidt, H.-A. Krug von Nidda, A. Loidl, and V. Tsurkan, Phys. Rev. Lett. **92**, 116401 (2004).
[7] N. Büttgen, J. Hemberger, V. Fritsch, A. Krimmel, M. Mücksch, H.-A. K. von Nidda, P. Lunkenheimer, R. Fichtl, V. Tsurkan, and A. Loidl, New J. Phys. **6**, 191 (2004).
[8] A. Krimmel, M. Mücksch, V. Tsurkan, M. M. Koza, H. Mutka, C. Ritter, D. V. Sheptyakov, S. Horn, and A. Loidl, Phys. Rev. B **73**, 014413 (2006).
[9] S. Giri, H. Nakamura, and T. Kohara, Phys. Rev. B **72**, 132404 (2005).
[10] N. Büttgen, A. Zymara, C. Kegler, V. Tsurkan, and A. Loidl, Phys. Rev. B **73**, 132409 (2006).
[11] G. Kalvius, O. Hartmann, D. Noakes, F. Wagner, R. Wäppling, U. Zimmermann, C. Baines, A. Krimmel, V. Tsurkan, and A. Loidl, Physica B (Amsterdam) **378-380**, 592 (2006).
[12] R. Fichtl, P. Lunkenheimer, J. Hemberger, V. Tsurkan, and A. Loidl, J. Non-Cryst. Solids **351**, 2793 (2005).
[13] A. Krimmel, H. Mutka, M. M. Koza, V. Tsurkan, and A. Loidl, Phys. Rev. B **79**, 134406 (2009).
[14] A. P. Ramirez, Annu. Rev. Mater. Sci. **24**, 453 (1994).
[15] A. P. Ramirez, in *Handbook of Magnetic Materials*, edited by K. H. J. Buschow (Elsevier, Amsterdam, 2001), Vol. 13, pp. 423–520.
[16] L. F. Feiner, A. M. Oles, and J. Zaanen, Phys. Rev. Lett. **78**, 2799 (1997).
[17] Y. Kitaoka, T. Kobayashi, A. Kōda, H. Wakabayashi, Y. Niino, H. Yamakage, S. Taguchi, K. Amaya, K. Yamaura, M. Takano, Atushi Hirano, and Ryoji Kanno, J. Phys. Soc. Jpn. **67**, 3703 (1998).
[18] M. V. Mostovoy and D. I. Khomskii, Phys. Rev. Lett. **89**, 227203 (2002).
[19] G. Chen, L. Balents, and A. P. Schnyder, Phys. Rev. Lett. **102**, 096406 (2009).
[20] K. Kugel and D. Khomskii, Sov. Phys. Usp. **25**, 231 (1982).
[21] T. Nikuni, M. Oshikawa, A. Oosawa, and H. Tanaka, Phys. Rev. Lett. **84**, 5868 (2000).
[22] M. Jaime, V. F. Correa, N. Harrison, C. D. Batista, N. Kawashima, Y. Kazuma, G. A. Jorge, R. Stern, I. Heinmaa, S. A. Zvyagin, Y. Sasago, and K. Uchinokura, Phys. Rev. Lett. **93**, 087203 (2004).
[23] K. Hida, J. Phys. Soc. Jpn. **61**, 1013 (1992).
[24] W. L. Roth, J. Phys. (Paris) **25**, 507 (1964).
[25] J. Vallin, Phys. Rev. B **2**, 2390 (1970).
[26] P. Chaikin and T. Lubensky, *Principles of Condensed Matter Physics* (Cambridge University Press, Cambridge, England, 1995).